Am J Clin Exp Urol 2019;7(4):215-222
www.ajceu.us /ISSN:2330-1910/AJCEU0099871

Original Article

Mri-based cancer lesion analysis with 3d printed patient specific prostate cutting guides

David R Rutkowski[1,2], Shane A Wells[2], Brian Johnson[3], Wei Huang[4], David F Jarrard[5], Joshua M Lang[6], Steve Cho[2], Alejandro Roldán-Alzate[1,2,3]

[1]Mechanical Engineering, [2]Radiology, [3]Biomedical Engineering, [4]Pathology, [5]Urology, [6]Medicine, University of Wisconsin, Madison, WI, United States

Received July 19, 2019; Accepted July 22, 2019; Epub August 15, 2019; Published August 30, 2019

Abstract: *Purpose:* MRI methods have improved diagnosis and treatment planning for prostate cancer. However, validation and standardization is needed to encourage widespread adoption of these methods. The purpose of this study was to improve validation methods by creating a prostate cutting guide and to develop a method for 3D comparison between MRI data and post-prostatectomy histological tissue slices. *Methods:* Prostate Specific Membrane Antigen (PSMA) Positron Emission Tomography (PET)/MRI was performed on 10 patients with prostate cancer before and after chemohormonal treatment. Post-treatment images were used to design patient-specific prostate cutting guides that were used to create uniform thickness sections of surgically removed prostates. The thickness of the prostate tissue slices matched the imaging slice thickness so that comparisons could be made between MRI results and histopathological study results. A method was also developed to compare post-slicing prostate bulk geometry with the predicted MRI prostate geometry. *Results:* The prostate cutting guides were used to successfully section the prostate for histopathogical evaluation and slice-by-slice MRI comparison. Surface comparison results displayed an average dimensional difference of 1.99 ± 3.19 mm between MRI and post-prostatectomy slice reconstruction prostate geometries. *Conclusion:* MRI-based prostate cutting guides were designed, fabricated, and implemented in a study examining the utility and accuracy of MRI for the detection of prostate cancer. Furthermore, a three-dimensional part comparison method was developed, which can be used for validation of MRI with pathological and histological data. Future work will analyze more subjects to examine the effectiveness of these guides for histopathological prostate analysis with MRI and PET/MRI.

Keywords: Magnetic resonance imaging, prostate cancer, 3D printing, prostatectomy

Introduction

Prostate cancer, one of the most common forms of cancer in America, affects nearly 165,000 men and leads to about 29,000 deaths annually [1]. Appropriate diagnosis and treatment planning for prostate cancer has historically been a challenge. However, recent advances in magnetic resonance imaging (MRI) methods have improved non-invasive detection and treatment planning of prostate cancer [2-4]. Yet, reliable standardization is still needed before large-scale implementation of multiparametric MRI in prostate cancer [5-8].

To improve reliability of MRI methods in prostate cancer detection, and move toward standardization, the spatial accuracy of MR prostate images must still be validated. This can be done through correlation between MRI and histopathology. However, a challenge in such an analysis is slice-by-slice comparison between MRI and the excised prostate. A number of studies have moved to address these issues through the use of MRI-based prostate cutting devices that allow for more accurate correlation between MRI data and histopathology data from excised prostates [9-14]. These devices provided stability and improved cutting accuracy and efficiency in both patient-specific [10] and multi-purpose [9, 13] designs. The purpose of this study was to work towards an improved cutting device for MRI validation and to develop a method for 3D comparison between pre-prostatectomy MRI data and post-prostatectomy histological slices.

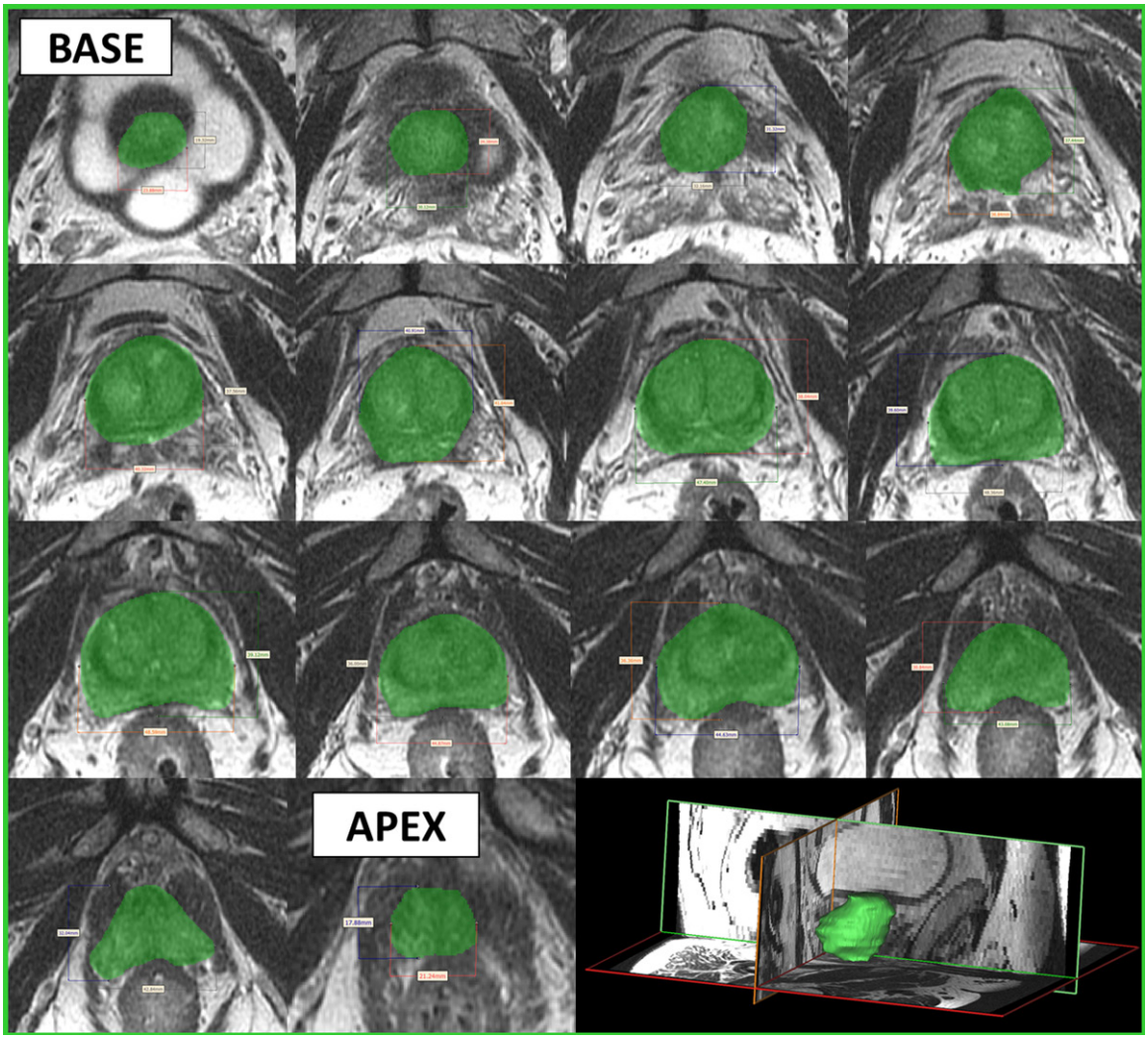

Figure 1. Axial-oblique T2-weighted prostate MRI obtained after chemohormonal therapy. Prior to prostatectomy, the prostate was contoured. These contours were used to create a 3D model of the prostate that would be used to generate a patient-specific cutting device for post-prostatectomy slicing.

Methods

Human subjects

10 patients with prostate cancer were prospectively recruited as part of a larger study analyzing histopathological and MRI methods for prostate cancer detection and treatment planning (ClinicalTrials.gov Identifiers: NCT03358563; NCT03232164).

Medical imaging

^{18}F-DCFPyL Prostate Specific Membrane Antigen (PSMA) Positron Emission Tomography (PET)/MRI (3T Signa PET/MR, GE Healthcare, Waukesha WI) was performed on the patients before and after neoadjuvant chemohormonal treatment. Both multiparametric prostate MRI and whole body MRI were performed. The post-treatment oblique axial T2-weighted images were oriented perpendicular to the subject urethra with a 260×247 mm field of view and an imaging slice thickness of 2.5 mm. These images were imported into MIMICS (Materialise, Leuven, Belgium), where the boundary of the prostate was contoured (DR) under the guidance of a fellowship-trained abdominal radiologist experienced in prostate imaging (SAW) (**Figure 1**). The prostate slice dimensions (width and height) were measured on each MR image slice and saved for later pathological investigation. The prostate surface was then interpolat-

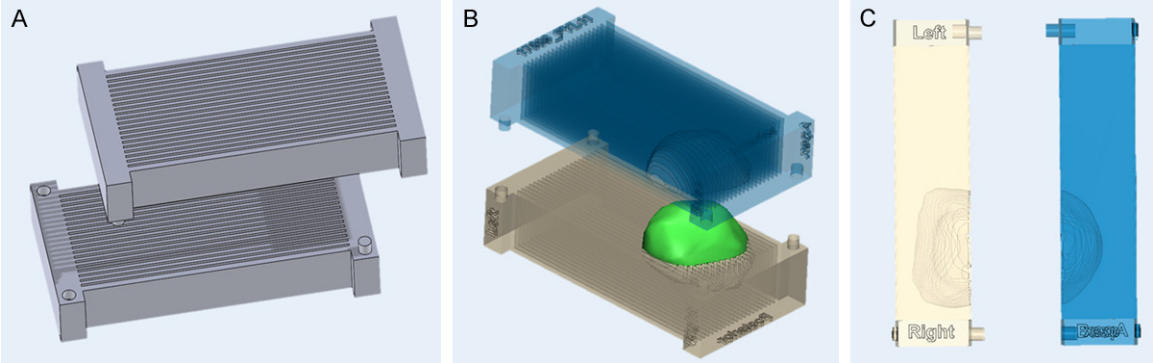

Figure 2. Patient-specific 3D cutting devices were created to section excised prostates for histopathological comparison. A. Device template to guide parallel 2.5 mm cuts in the prostate. B. Patient-specific prostate geometry subtracted from the device template. C. Labeled prostate cutting device showing the internal prostate contours.

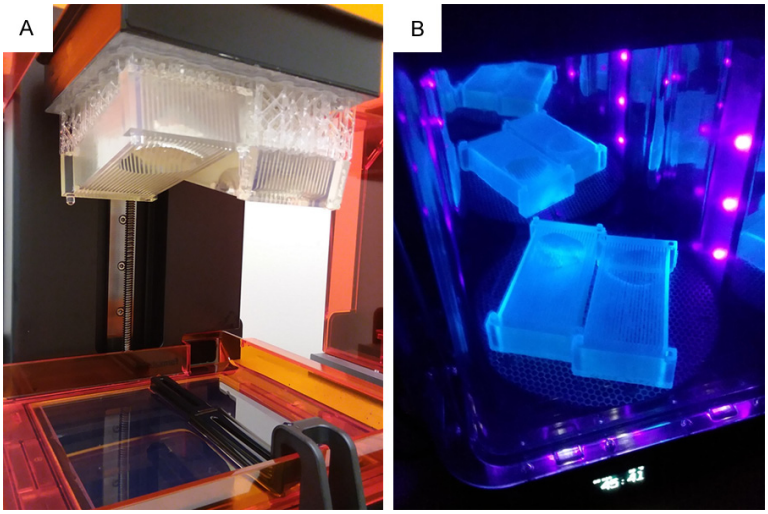

Figure 3. The MRI-based molds were fabricated with an additive manufacturing method. A. The two halves of the mold were printed with a stereolitography machine. B. The mold components were soaked in isopropyl alcohol and cured in UV light to improve surface finish and sterilize the mold.

ed between MR image slices and a 3D volume was generated.

Prostate slicing guide design

To create a guide that allows for consistent cutting of the prostate at 2.5 mm increments, a guide template was designed in Solidworks (Dassault Systèmes, Waltham, MA), as shown in **Figure 2A**. The guide design consisted of twenty-two 10 cm-long, 1 mm thick, openings arranged in a parallel orientation. The length of the slots allowed for effective slicing all the way through the prostate specimen. These slots were anchored with solid perpendicular supports at each end of the guide device. Both ends of the guide device contained either a pin or a pin slot that served the purpose of holding each half of the mold in the proper orientation. To avoid improper alignment of the two device halves, pins and pin slots were alternated.

After creating the slicing guide template, the mold designs were made patient specific. To do this, both the guide device template and the segmented patient-specific prostate 3D surface were imported into 3-matic design software. The patient specific prostate surface was oriented in a way that aligned the guide slots perpendicular to the urethra direction on the prostate, allowing for precise co-registration with the oblique axial T2-weighted images. The surface was then subtracted from the mold template volume (**Figure 2B**), leaving a void for the excised prostate. The mold was then labeled with the patient study number and anterior/posterior, right/left, and base/apex notations (**Figure 2C**).

Prostate slicing guide fabrication and preparation

To fabricate the guide, the patient-specific 3D model was exported to a steriolothography additive manufacturing machine (Form2, Formlabs, Somerville, MA) (**Figure 3**). This machine

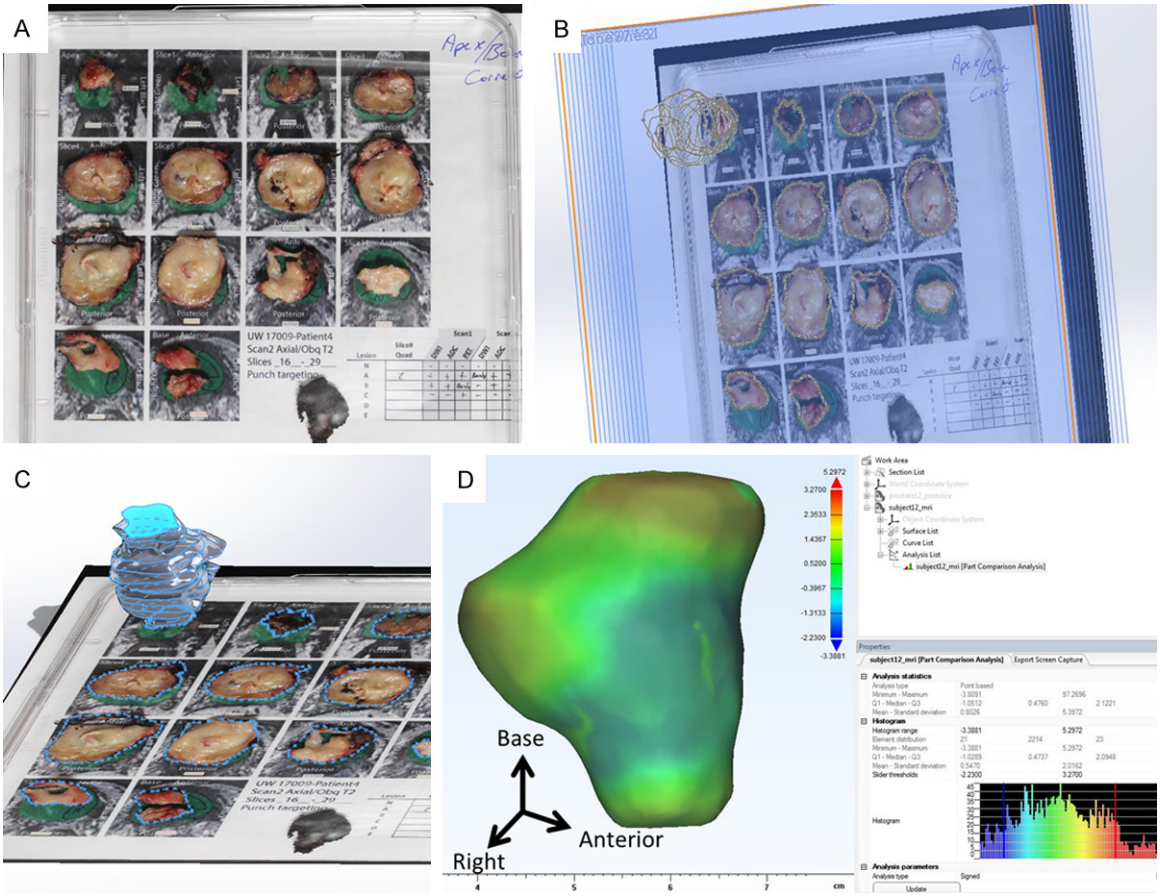

Figure 4. After sectioning, the prostate slices were (A) placed on images of the pre-prostatectomy MRI contours. (B) Virtual outlines of the prostate slices were stacked in 2.5 mm increments to (C) loft the contours and create a representative post-prostatectomy 3D geometry for (D) surface comparison analysis with the original MRI-segmented prostate model.

used a photopolymer resin to build both halves of the patient-specific device in a layer-wise fashion. The build for each half of the patient-specific device took approximately 12 hours. When the print was finished, it was cleaned in isopropyl alcohol for 15 minutes and then cured in a UV light heating chamber for 30 minutes.

Prostate slicing

The finished guide was taken to the institution's surgical pathology grossing room. Here, the device was sterilized by briefly (<1 minute), soaking it in 70% ethanol alcohol and then exposing it to UV light irradiation for 15-30 minutes. Once sterilized, the mold was used to section the prostate. To do this, the excised prostate was placed in the first half of the patient-specific device void and oriented to match the guide device anatomical labels. The second half of the device was then positioned and the device was turned vertically. A tissue slicer blade (Thomas Scientific, Swedesboro, NJ) was then run through each slot of the device to cut the prostate tissue at the predefined increments. The prostate slices were then oriented on the MRI-derived 2D contours, as shown in **Figure 4A**, and a picture was taken for later analysis.

Geometric analysis

To analyze the 3D accuracy of the MRI-based prostate mold, the post-resection prostate volume was reconstructed based on the prostate slices from surgical pathology. To do this, contours of the prostate slices were stacked on planes 2.5 mm apart (**Figure 2B**), and lofted to create a 3D volume in Solidworks (**Figure 4C**). The 3D surface was then imported into 3-matic, along with the MRI-based 3D surface. A part comparison analysis was then performed to

Table 1. Statistics for surface point comparison between pre-prostatectomy MRI and post-prostatecomy slice reconstruction prostate geometries

Subject	Q1 (mm)	Median (mm)	Q3 (mm)	Mean (mm)	Standard Deviation (mm)
1	-0.72	0.85	2.39	1.16	2.37
2	-2.51	-0.99	0.94	-1.05	2.35
3	2.10	3.42	5.08	3.62	1.98
4	1.81	3.32	5.06	3.25	2.16
5	0.53	0.53	0.53	0.57	0.35
6	2.07	3.12	4.28	3.21	1.58
7	0	1.99	2.31	2	2.38
8	-0.21	1.43	3.67	2.17	3.34
9	1.20	3.09	5.30	4.2	9.91
10	-1.05	0.47	2.12	0.80	5.39
Average	0.32	1.73	3.17	1.99	3.19

generate regional difference maps comparing the MRI-derived prostate geometry with the representative post-prostatectomy geometry (**Figure 4D**).

Results

The patient-specific guides were used to effectively slice the unfixed prostate at 2.5 mm increments (**Figure 4A**). However, some slice sections were occasionally warped after cutting. This was presumed to be due to an anisotropic pressure build-up inside the resected prostate due to hyperplasia. Nonetheless, computer reconstruction of the post-prostatectomy prostate was successful for each of the ten patients.

The post-prostatectomy reconstructed volumes were, on average, 1.99 mm (±3.19 mm) smaller than the pre-prostatectomy MRI-based volume. This was based on point-to-point surface comparison, and lies below the imaging slice resolution of 2.5 mm. These measurements were associated with a moderate amount of patient-specific variation, as displayed in **Table 1** and **Figure 5**. Note that pre-prostatectomy MRI to post-prostatectomy reconstruction surface differences ranged anywhere from -2.51 mm to 5.08 mm. Note also the unique shapes produced by post-slice reconstruction, compared to MRI, as shown in **Figure 5**.

Iteration in the guide device fabrication and sterilization process also produced some unique results. It was found that when the device was sterilized in ethanol alcohol for longer than 1-2 hours before entering the grossing room, the long narrow slots on the device experienced significant warpage, as shown in **Figure 6**. This rendered the device unusable and irreparable. However, when sterilized for 15 minutes or less in an isopropyl alcohol solution, the material used for these devices was not degraded.

Discussion

In this study, we demonstrated the feasibility of creating three-dimensional patient specific cutting guides that allowed for slice-by-slice comparison of whole-mount histopathology slices/slides to T2-weighted MRI images. Furthermore, a three-dimensional analysis method was developed that allowed for qualitative and quantitative comparison between MRI-segmented prostate dimensions with post-prostatectomy prostate dimensions.

The motivation for this study was MRI cancer detection. MRI has already demonstrated valuable clinical utility in detection and treatment planning of prostate cancer. However, to increase reliability, methods must be validated and standardized. In an effort to validate MRI diagnostic methods for the prostate, pre-prostatectomy MRI data can be compared with post-prostatectomy histopathological prostate slices. Devices that aid in repeatable and accurate cutting of the prostate can help move studies toward standardization. Slice-by-slice comparison of pre-surgery MRI and post-prostatectomy tissue is very important for other reason as well. It not only has the potential to improve the reading of prostate MRI, but also may help improve the quality of the MRI, and therefore improve cancer detection. The methods used in this study, in particular, led to a better understanding of the utility of PSMA in prostate cancer detection.

The majority of this work is focused on the development and application of the prostate cutting guides. To date, a number of factors have been noted that affect imaged-based

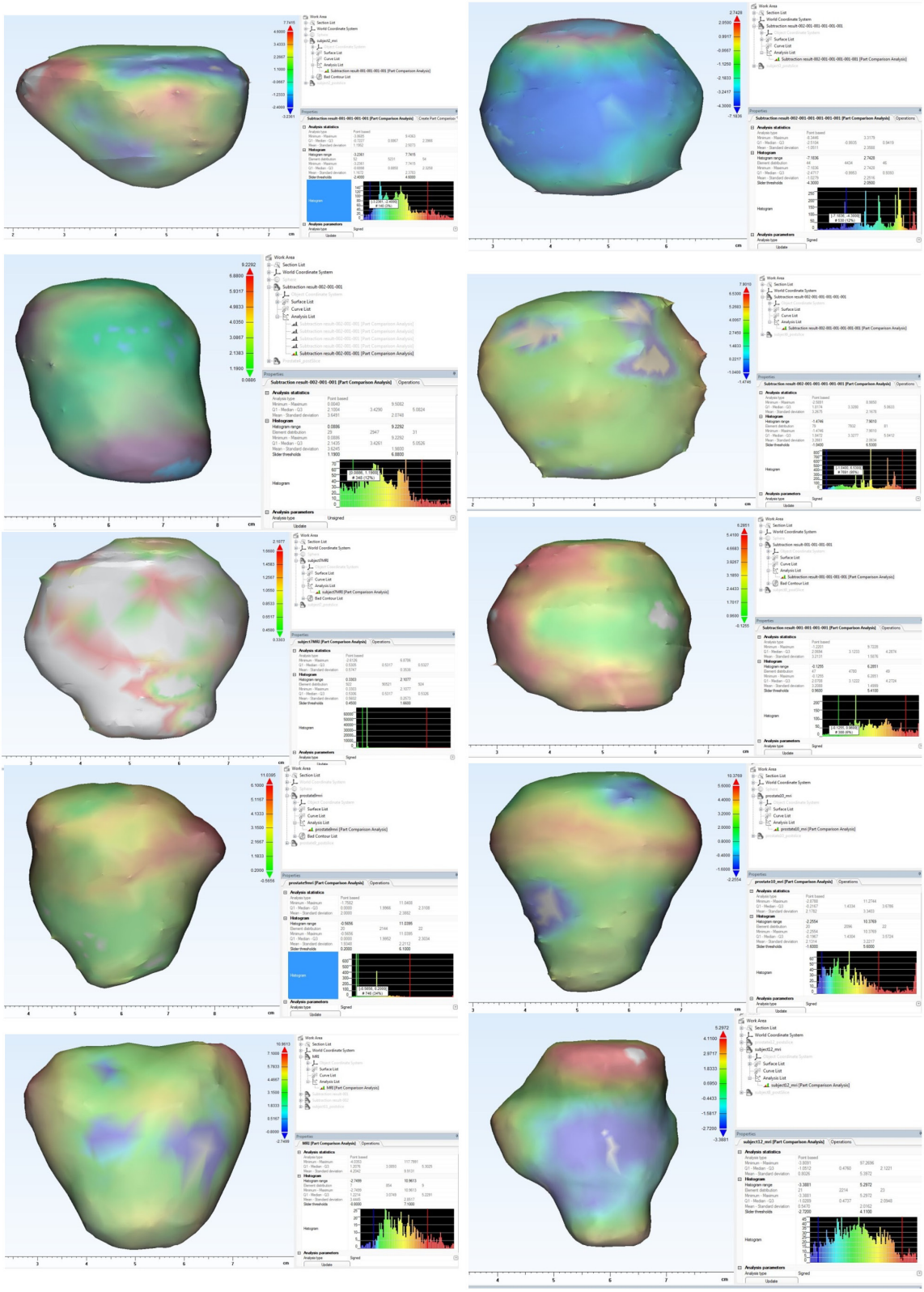

Figure 5. Comparison between pre-prostatectomy MRI and post-prostatecomy slice reconstruction prostate geometries.

prostate cutting guide performance [3]. First of all, the fit of the device to the resected prostate can have implications on quality and efficiency of tissue partitioning. A holder that does not

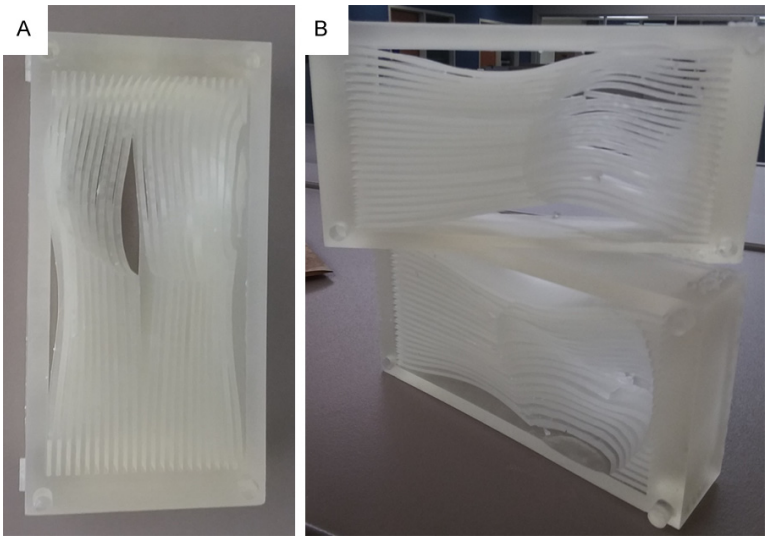

Figure 6. Device knife slot warpage after being sterilized in alcohol for longer than 1-2 hours.

dimensions of the prostate, the prostate was sliced immediately after it was surgically removed (within 1 hour). This way, minimal time was allowed for additional drying and deformation of the harvested tissue. We would like to note that post-prostatectomy analyses often involve formalin fixation, which can lead to shrinking of the prostate before it is cut. However, if the prostate is resected and sliced on the same day, then a patient-specific guide designed with MRI data can be a valuable tool for accurate MRI to histopathology comparison.

firmly grip the specimen and guide the knife at evenly spaced increments will result in non-uniform slice thicknesses and inhibit accurate comparison with MRI slice segments. Accordingly, this study employed patient-specific cutting devices based upon individualized prostate contours. This provided a firm hold on the tissue specimen as the knife was run through the pre-designed slots. Another consideration in creating a prostate tissue cutting guide is the thickness of the MR image slices. Previous studies administered MRI procedures at a slice spacing of 3-6 mm. In an effort to improve pre- to post-prostatectomy comparison, and in order to provide more tissue samples to histology, this study used a slice thickness of 2.5 mm. This not only helped in definition of a more representative void in the cutting device, but also provided more data points for post-slicing virtual prostate reconstruction.

One issue that was encountered in the post-prostatectomy analysis process was slice deformation after cutting. This was presumed to be a result of knife deflection around hard benign prostate hyperplasia nodules. Furthermore, changes in the prostate size and volume as a whole would occasionally occur after resection, creating a difference between the size predicted by MRI and the size of the ex-vivo prostate. This would certainly affect post-prostatectomy virtual reconstruction results. To avoid this issue, and others that may affect the

Iterations in the fabrication and sterilization process also produced some results that were used to improve future device design and fabrication. First, multiple additive manufacturing (3D printing) techniques were tested, which included fused deposition modeling (FDM), powder bed fusion/selective laser sintering, and vat photo-polymerization/stereolithography (SLA). Of these three methods, FDM and SLA produced the most time- and cost-effective cutting devices while still providing functional equivalence. Past studies have relied on FDM techniques to print similar devices for prostate sectioning. However, in this work, SLA was chosen as the go-to method because of its shorter build times (useful for short turn-around between MRI and prostatectomy dates) and higher surface quality. Furthermore, minimal post-processing was required with the SLA method. Nonetheless, one necessary post-processing precaution that was learned from this study was the limits on alcohol sterilization. Although the SLA method required an alcohol rinse on the device after the build was complete, repeated alcohol exposure proved detrimental to the structure of the parallel slots on the device. Therefore, during alcohol sterilization that occurs before prostate sectioning, it is recommended to expose the device to alcohol for no longer than 15 minutes.

In conclusion, a MRI-based prostate cutting guide was designed, fabricated, and implemented into a study examining the utility and

accuracy of MRI for the location and diagnosis of prostate cancer. Furthermore, a three-dimensional part comparison method was developed, which can be used for validation of MRI with pathological and histological data. Future work will analyze more subjects to examine the effectiveness of these devices for histopathological prostate analysis with MRI and PET/MRI.

Acknowledgements

The research presented was supported by the NIH (UL1TR000427, TL1TR000429) and DOD IMPACT award PC15053. The authors also wish to acknowledge support from GE Healthcare who provides research support to the University of Wisconsin.

Disclosure of conflict of interest

None.

Address correspondence to: David R Rutkowski and Alejandro Roldán-Alzate, Mechanical Engineering, University of Wisconsin, Madison, WI, United States. E-mail: drutkowski2@wisc.edu (DRR); roldan@wisc.edu (ARA)

References

[1] Prostate Cancer Facts. Prostate Cancer Foundation; 2018.

[2] Pathmanathan AU, McNair HA, Schmidt MA, Brand DH, Delacroix L, Eccles CL, Gordon A, Herbert T, van As NJ, Huddart RA, Tree AC. Comparison of prostate delineation on multimodality imaging for MR-guided radiotherapy. Br J Radiol 2019; 92: 20180948.

[3] Kim R, Kim CK, Park JJ, Kim JH, Seo SI, Jeon SS, Lee HM. Prognostic significance for long-term outcomes following radical prostatectomy in men with prostate cancer: evaluation with prostate imaging reporting and data system version 2. Korean J Radiol 2019; 20: 256-264.

[4] Parra NA, Lu H, Li Q, Stoyanova R, Pollack A, Punnen S, Choi J, Abdalah M, Lopez C, Gage K, Park JY, Kosj Y, Pow-Sang JM, Gillies RJ, Balagurunathan Y. Predicting clinically significant prostate cancer using DCE-MRI habitat descriptors. Oncotarget 2018; 9: 37125-37136.

[5] Wang M, Janaki N, Buzzy C, Bukavina L, Mahran A, Mishra K, MacLennan G, Ponsky L. Whole mount histopathological correlation with prostate MRI in Grade I and II prostatectomy patients. Int Urol Nephrol 2019; 51: 425-434.

[6] Mehralivand S, Shih JH, Harmon S, Smith C, Bloom J, Czarniecki M, Gold S, Hale G, Rayn K, Merino MJ, Wood BJ, Pinto PA, Choyke PL, Turkbey B. A grading system for the assessment of risk of extraprostatic extension of prostate cancer at multiparametric MRI. Radiology 2019; 290: 181278.

[7] Eberhardt SC. Local staging of prostate cancer with MRI: a need for standardization. Radiology 2019; 290: 182943.

[8] Diamand R, Oderda M, Al Hajj Obeid W, Albisinni S, Van Velthoven R, Fasolis G, Simone G, Ferriero M, Roche JB, Piechaud T, Pastore A, Carbone A, Fiard G, Descotes JL, Marra G, Gontero P, Altobelli E, Papalia R, Kumar P, Eldred-Evans D, Giacobbe A, Muto G, Lacetera V, Beatrici V, Roumeguere T, Peltier A. A multicentric study on accurate grading of prostate cancer with systematic and MRI/US fusion targeted biopsies: comparison with final histopathology after radical prostatectomy. World J Urol 2019; [Epub ahead of print].

[9] Drew B, Jones EC, Reinsberg S, Yung AC, Goldenberg SL, Kozlowski P. Device for sectioning prostatectomy specimens to facilitate comparison between histology and in vivo MRI. J Magn Reson Imaging 2010; 32: 992-996.

[10] Shah V, Pohida T, Turkbey B, Mani H, Merino M, Pinto PA, Choyke P, Bernardo M. A method for correlating in vivo prostate magnetic resonance imaging and histopathology using individualized magnetic resonance-based molds. Rev Sci Instrum 2009; 80: 104301.

[11] Jackson AS, Reinsberg SA, Sohaib SA, Charles-Edwards EM, Jhavar S, Christmas TJ, Thompson AC, Bailey MJ, Corbishley CM, Fisher C, Leach MO, Dearnaley DP. Dynamic contrast-enhanced MRI for prostate cancer localization. Br J Radiol 2009; 82: 148-156.

[12] Kimm SY, Tarin TV, Lee JH, Hu B, Jensen K, Nishimura D, Brooks JD. Methods for registration of magnetic resonance images of ex vivo prostate specimens with histology. J Magn Reson Imaging 2012; 36: 206-212.

[13] Yamamoto H, Nir D, Vyas L, Chang RT, Popert R, Cahill D, Challacombe B, Dasgupta P, Chandra A. A workflow to improve the alignment of prostate imaging with whole-mount histopathology. Acad Radiol 2014; 21: 1009-1019.

[14] Hughes C, Rouvière O, Mege-Lechevallier F, Souchon R, Prost R. Robust alignment of prostate histology slices with quantified accuracy. IEEE Trans Biomed Eng 2013; 60: 281-291.